Article

Calcium Binding and Head Group Dipole Angle in Phosphatidylserine#Phosphatidylcholine Bilayers

P. Thomas Vernier, Matthew J. Ziegler, and Rumiana Dimova

Langmuir, **2009**, 25 (2), 1020-1027 • DOI: 10.1021/la8025057 • Publication Date (Web): 08 December 2008

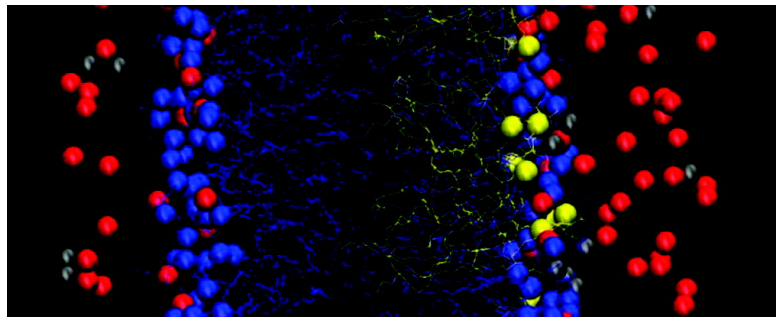

Calcium Binding and Head Group Dipole Angle in Phosphatidylserine−Phosphatidylcholine Bilayers

P. Thomas Vernier,*,† Matthew J. Ziegler,‡ and Rumiana Dimova§

Ming Hsieh Department of Electrical Engineering and Mork Family Department of Chemical Engineering and Materials Science, Viterbi School of Engineering, University of Southern California, Los Angeles, California 90089-0271, and Department of Theory and Bio-Systems, Max Planck Institute of Colloids and Interfaces, Science Park Golm, 14424 Potsdam, Germany

Received August 2, 2008. Revised Manuscript Received October 31, 2008

Manipulating the plasma membrane, the gateway to the cell interior, with chemical and physical agents for genetic and pharmacological therapy, and understanding the interactions of lipid membrane components with proteins and other structural and functional elements of the cell, require a detailed biomolecular membrane model. We report here progress along one path toward such a model: molecular dynamics simulations of mixed, zwitterionic-anionic, asymmetric phospholipid bilayers with monovalent and divalent cations. With phosphatidylcholine/phosphatidylserine systems, we identify temporal and concentration boundaries for equilibration of calcium with the bilayer and saturation of the calcium capacity of the membrane, we demonstrate the electrostatic- and entropic-driven associations of calcium and sodium ions with polar groups in the bilayer interface region, expressed in spatial distribution profiles and in changes in the orientation of the phospholipid head groups, and we describe for the first time simulations of dynamic, calcium-mediated adjustments in the conformation of mixed phospholipid species coresident in the same leaflet of the bilayer. The results are consistent with experimental observations and point the way to further refinement and increased realism of these molecular models.

1. Introduction

The complex biophysical landscape of cell membranes reflects the functions of partition, transport, and communication that define the instant physiological state of the cell. Considerable effort has been devoted to understanding the detailed structure and dynamic organization of this nanoscale barrier,[1] using living cells, model membranes, and computer simulations. Atomic-resolution molecular dynamics (MD) simulations of lipid bilayers have contributed to our knowledge of the kinetics and energetics of molecular interactions in the membrane and at the aqueous interface, and in recent years the expansion of available computational power has enabled the practical analysis of larger systems (hundreds of lipid and thousands of water molecules) for longer times (hundreds of nanoseconds), so that we can now see beyond snapshots of conformation to events of cell biological significance such as the operation of ion channels[2] or the electroporation of the membrane.[3]

We present here the results of MD simulations of asymmetric phospholipid bilayers composed of dioleoylphosphatidylcholine (DOPC) in one leaflet and a mixture of DOPC and dioleoylphosphatidylserine (DOPS) in the other leaflet, with calcium, sodium, and chloride ions in the aqueous medium, a simple representation of the configuration in living cell membranes. The interaction of calcium with phospholipid bilayers in general, and with anionic phospholipids such as DOPS in particular, is of interest because of the role of calcium ion gradients in a wide variety of cell physiological processes[4] and because of the importance of anionic phospholipid localization in cell signaling[5−7] and structuring of the membrane.[8,9]

Experimental investigations of phospholipid bilayer stacks and vesicles in aqueous electrolytes have shown that the properties of these systems are highly dependent on the specific ions present and their concentration,[10] and that measured values for the calcium binding constant,[10−19] calcium/phospholipid stoichiometry,[10,12,13,15,20,21] and headgroup dipole angle[11,22,23] can vary, in some cases over a wide range, for different phospholipids and analytical techniques. MD simulations of phospholipid bilayers have yielded results generally consonant with these observations

* Corresponding author. E-mail: vernier@usc.edu.
† Ming Hsieh Department of Electrical Engineering, University of Southern California.
‡ Mork Family Department of Chemical Engineering and Materials Science, University of Southern California.
§ Max Planck Institute of Colloids and Interfaces.

(1) Jacobson, K.; Mouritsen, O. G.; Anderson, R. G. *Nat. Cell Biol.* **2007**, *9*(1), 7–14.
(2) Jogini, V.; Roux, B. *Biophys. J.* **2007**, *93*(9), 3070–82.
(3) Tieleman, D. P. *BMC Biochem.* **2004**, *5*(1), 10.
(4) Berridge, M. J.; Bootman, M. D.; Roderick, H. L. *Nat. Rev. Mol. Cell Biol.* **2003**, *4*(7), 517–29.
(5) Fadok, V. A.; de Cathelineau, A.; Daleke, D. L.; Henson, P. M.; Bratton, D. L. *J. Biol. Chem.* **2001**, *276*(2), 1071–7.
(6) Elliott, J. I.; Surprenant, A.; Marelli-Berg, F. M.; Cooper, J. C.; Cassady-Cain, R. L.; Wooding, C.; Linton, K.; Alexander, D. R.; Higgins, C. F. *Nat. Cell Biol.* **2005**, *7*(8), 808–16.
(7) Yeung, T.; Gilbert, G. E.; Shi, J.; Silvius, J.; Kapus, A.; Grinstein, S. *Science* **2008**, *319*(5860), 210–3.
(8) Tanaka, Y.; Schroit, A. J. *Biochemistry* **1986**, *25*(8), 2141–8.
(9) Pedersen, U. R.; Leidy, C.; Westh, P.; Peters, G. H. *Biochim. Biophys. Acta* **2006**, *1758*(5), 573–82.
(10) McLaughlin, S.; Mulrine, N.; Gresalfi, T.; Vaio, G.; McLaughlin, A. *J Gen Physiol* **1981**, *77*(4), 445–73.
(11) Akutsu, H.; Seelig, J. *Biochemistry* **1981**, *20*(26), 7366–73.
(12) Altenbach, C.; Seelig, J. *Biochemistry* **1984**, *23*(17), 3913–20.
(13) Feigenson, G. W. *Biochemistry* **1986**, *25*(19), 5819–25.
(14) Tatulian, S. A. *Eur. J. Biochem.* **1987**, *170*(1−2), 413–20.
(15) Mattai, J.; Hauser, H.; Demel, R. A.; Shipley, G. G. *Biochemistry* **1989**, *28*(5), 2322–30.
(16) Feigenson, G. W. *Biochemistry* **1989**, *28*(3), 1270–8.
(17) Seelig, J. *Cell Biol. Int. Rep* **1990**, *14*(4), 353–60.
(18) Binder, H.; Zschornig, O. *Chem. Phys. Lipids* **2002**, *115*(1−2), 39–61.
(19) Pabst, G.; Hodzic, A.; Strancar, J.; Danner, S.; Rappolt, M.; Laggner, P. *Biophys. J.* **2007**, *93*(8), 2688–96.
(20) Herbette, L.; Napolitano, C. A.; McDaniel, R. V. *Biophys. J.* **1984**, *46*(6), 677–85.
(21) Huang, J.; Swanson, J. E.; Dibble, A. R.; Hinderliter, A. K.; Feigenson, G. W. *Biophys. J.* **1993**, *64*(2), 413–25.
(22) Seelig, J.; Macdonald, P. M.; Scherer, P. G. *Biochemistry* **1987**, *26*(24), 7535–41.
(23) Clarke, R. J.; Lupfert, C. *Biophys. J.* **1999**, *76*(5), 2614–24.

10.1021/la8025057 CCC: $40.75
Published on Web 12/08/2008

for binding constant,[9,24−28] stoichiometry,[9] and headgroup dipole angle.[26,29−31]

A recent experimental study[32] of calcium binding to phosphatidylcholine−phosphatidylserine (PC:PS) vesicles addresses the spread of published values for the binding constant of calcium to phospholipid bilayers with a systematic physical analysis under controlled conditions of ionic strength and osmolarity. These results make clear the importance of the ion spatial distribution profile and associated electrostatics for modeling calcium binding to phospholipid bilayers. The ions that bind to the membrane interface partition from the local concentration adjacent to the membrane, not from the bulk, and the differential can be quite large (a factor of 100 or more).[17] The data of Sinn et al. suggest that it is this high surface calcium concentration, driven by electrostatics, not a preferential attraction to PS, that accounts for the greater observed binding of calcium to PC:PS vesicles relative to those composed of pure PC. They also provide evidence that calcium binding to vesicles is entropy-driven (and endothermic), and suggest that the entropy increase results from the loss of some water from the calcium hydration shell for membrane-bound calcium ions and, at the same time, a calcium-mediated dehydration of the lipid membrane (calcium replaces some water in the membrane interface).

We place our simulations of mixed-composition phospholipid bilayers with calcium in the context of these experimental results and of previously reported MD simulations of lipid membranes with aqueous electrolytes. We report lipid area and headgroup dipole angle effects, detailed atomic density profiles, radial distribution functions, and equilibrium binding distributions of calcium and water in the membrane interfacial region for bilayer systems containing: 128 phospholipids (DOPC:DOPS = 128:0, 118:10, 108:20), with all of the DOPS molecules in one leaflet of the bilayer in each case, to represent the normal asymmetric distribution in cell membranes; 0, 10, and 100 ionized $CaCl_2$ molecules; 0, 10, and 20 Na^+ counterions for the anionic DOPS residues; and 4180−4480 water molecules. For pure DOPC and for mixed, asymmetric DOPC:DOPS systems, we observe calcium-induced structural changes, binding kinetics and distribution, and stoichiometry that are generally consistent with previous work, and we describe for the first time the interacting and opposing effects of calcium and the anionic phospholipid PS on the properties of DOPC:DOPS bilayers, including the PC headgroup dipole angle.

2. Simulation Methods

MD Simulations. All simulations were performed using the GroMACS set of programs version 3.3.1[33−35] on the University of Southern California High Performance Computing and Communications Linux cluster (http://www.usc.edu/hpcc/). Lipid parameters for DOPC were derived from the OPLS, united-atom parameters of Berger et al.[3,36] Additional headgroup parameters and charges for PS were taken from Mukhopadhyay et al.[37] or were provided by D. P. Tieleman (personal communication). The simple point charge (SPC) model[38] for water was chosen for compatibility with the lipid models, computational advantages, and the ability to produce the correct area per lipid. Systems were coupled to a temperature bath at 310 K with a relaxation time of 0.1 ps and a pressure bath at 1 bar with a relaxation time of 1 ps, each using a weak coupling algorithm.[39] Pressure was scaled semi-isotropically with a compressibility of 4.5×10^{-5} bar^{-1} in the plane of the membrane and 4.5×10^{-5} bar^{-1} perpendicular to the membrane. Bond lengths were constrained using LINCS[40] for lipids and SETTLE[41] for water. Short-range electrostatics and Lennard-Jones interactions were cut off at 1.0 nm. Long-range electrostatics were calculated by the particle mesh Ewald (PME) algorithm[42] using fast Fourier transforms and conductive boundary conditions. Real-space interactions were cut off at 1.0 nm, and reciprocal-space interactions were evaluated on a 0.12 nm grid with fourth-order B-spline interpolation. The parameter ewald_rtol, which controls the relative error for the Ewald sum in the direct and reciprocal space, was set to 10^{-5}. Periodic boundary conditions were employed to mitigate system size effects.

Asymmetric bilayer systems, particularly those with anionic phospholipids in one leaflet, are of interest as a beginning approximation to the configuration of many biological membranes. The systems we use are stable, as judged by area per lipid and by the maintenance of the integrity and planarity of the bilayer, over hundreds of nanoseconds. No tendency toward curvature or bending, which one might expect in an asymmetric bilayer, appears, even over these relatively long simulation times. Although we see no indication that any unbalanced mechanical force is affecting the outcome of the simulations reported in this paper, we anticipate a need to compensate for the asymmetry in the larger systems to be investigated in future work.

Structures. A sample DOPC lipid structure was obtained from the Protein Data Bank (http://www.rcsb.org/), and custom code was used to create a bilayer system with 128 DOPC and 4480 water molecules (35 waters per lipid). The system was equilibrated until the area per lipid was constant. Using custom code and the GroMACS function genion, nine systems were created from the pure DOPC system, summarized in Table 1.

For systems with DOPS, custom code was used to substitute a DOPS for a DOPC by modifying the headgroup and adding a corresponding sodium counterion. A short 10 ps equilibration was performed to test each lipid substitution for bad contacts. For systems with calcium, the GroMACS function genion was used to place ions. Genion intelligently replaces a random solvent water molecule with an ion in a low energy environment and does not require further equilibration. For example, in order to add $CaCl_2$, three random water molecules are removed and replaced by calcium and chloride ions.

(24) Pandit, S. A.; Berkowitz, M. L. *Biophys. J.* **2002**, *82*(4), 1818–27.
(25) Bockmann, R. A.; Hac, A.; Heimburg, T.; Grubmuller, H. *Biophys. J.* **2003**, *85*(3), 1647–55.
(26) Bockmann, R. A.; Grubmuller, H. *Angew. Chem., Int. Ed. Engl.* **2004**, *43*(8), 1021–4.
(27) Shinoda, K.; Shinoda, W.; Mikami, M. *Phys. Chem. Chem. Phys.* **2007**, *9*(5), 643–50.
(28) Zhao, W.; Rog, T.; Gurtovenko, A. A.; Vattulainen, I.; Karttunen, M. *Biophys. J.* **2007**, *92*(4), 1114–24.
(29) Pandit, S. A.; Bostick, D.; Berkowitz, M. L. *Biophys. J.* **2003**, *85*(5), 3120–31.
(30) Sachs, J. N.; Nanda, H.; Petrache, H. I.; Woolf, T. B. *Biophys. J.* **2004**, *86*(6), 3772–82.
(31) Hogberg, C. J.; Lyubartsev, A. P. *Biophys. J.* **2008**, *94*(2), 525–31.
(32) Sinn, C. G.; Antonietti, M.; Dimova, R. *Colloids Surf., A: Physicochem. Eng. Aspects* **2006**, *282*, 410–419.
(33) Berendsen, H. J. C.; van der Spoel, D.; van Drunen, R. *Comput. Phys. Commun.* **1995**, *91*(1−3), 43–56.
(34) Lindahl, E.; Hess, B.; van der Spoel, D. *J. Mol. Model.* **2001**, *7*(8), 306–317.
(35) van der Spoel, D.; Lindahl, E.; Hess, B.; Groenhof, G.; Mark, A. E.; Berendsen, H. J. *J. Comput. Chem.* **2005**, *26*(16), 1701–18.
(36) Berger, O.; Edholm, O.; Jahnig, F. *Biophys. J.* **1997**, *72*(5), 2002–13.
(37) Mukhopadhyay, P.; Monticelli, L.; Tieleman, D. P. *Biophys. J.* **2004**, *86*(3), 1601–9.
(38) Berendsen, H. J. C.; Postma, J. P. M.; van Gunsteren, W. F.; Hermans, J. Interaction models for water in relation to protein hydration. In *Intermolecular Forces*; Pullman, B., Ed. Reidel: Dordrecht, Netherlands, 1981; pp 331−342.
(39) Berendsen, H. J. C.; Postma, J. P. M.; van Gunsteren, W. F.; Dinola, A.; Haak, J. R. *J. Chem. Phys.* **1984**, *81*(8), 3684–3690.
(40) Hess, B.; Bekker, H.; Berendsen, H. J. C.; Fraaije, J. G. E. M. *J. Comput. Chem.* **1997**, *18*(12), 1463–1472.
(41) Miyamoto, S.; Kollman, P. A. *J. Comput. Chem.* **1992**, *13*(8), 952–962.
(42) Essmann, U.; Perera, L.; Berkowitz, M. L.; Darden, T.; Lee, H.; Pedersen, L. G. *J. Chem. Phys.* **1995**, *103*(19), 8577–8593.

Table 1. System Configurations

	outer (left) leaflet	inner (right) leaflet		ions			
system name	DOPC	DOPC	DOPS	calcium	sodium	chloride	water
0 PS 0 Ca	64	64	0	0	0	0	4480
0 PS 10 Ca	64	64	0	10	0	20	4450
0 PS 100 Ca	64	64	0	100	0	200	4180
10 PS 0 Ca	64	54	10	0	10	0	4480
10 PS 10 Ca	64	54	10	10	10	20	4450
10 PS 100 Ca	64	54	10	100	10	200	4180
20 PS 0 Ca	64	44	20	0	20	0	4480
20 PS 10 Ca	64	44	20	10	20	20	4450
20 PS 100 Ca	64	44	20	100	20	200	4180

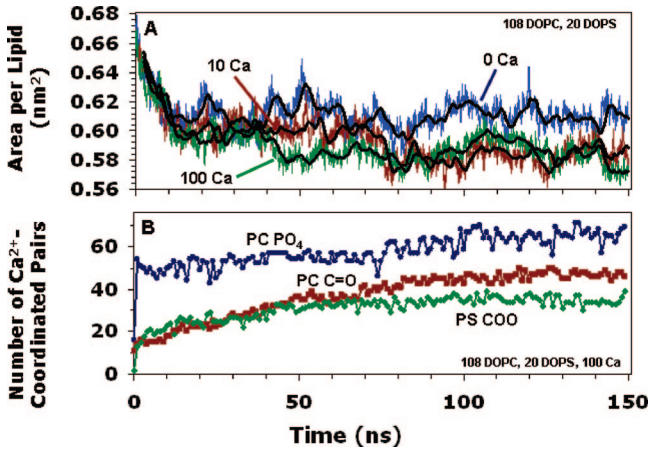

Figure 1. (A) Area per lipid as a function of time for a DOPC:DOPS (108:20) system. Adding calcium to the system results in tighter lipid packing and a decrease in the bilayer area. Data points every 10 ps. Heavy lines are a 2.5 ns moving average. (B) Number of calcium−oxygen coordinated pairs (calcium−phosphatidyl (PO_4), calcium−carbonyl (C═O), calcium−carboxyl (COO)) as a function of time for a DOPC:DOPS (108:20) system containing 100 calcium ions. Binding stabilizes after about 100 ns.

Calcium Binding Criteria. Criteria for binding of calcium to other atom groups are similar to those used in simulations of calcium binding to palmitoyloleoylphosphatidylcholine (POPC).[26] A radial distribution function was created by calculating the distance between each calcium ion and the phosphatidyl, carbonyl, and carboxyl oxygens in the system. Atoms closer than 0.3 nm are considered bound. No binding was observed between calcium and nitrogen or calcium and phosphorus.

Images. Molecular graphics images were generated with visual molecular dynamics (VMD).[43]

3. Results and Discussion

System Equilibration Time, Area Per Lipid, Bilayer Thickness. Establishment of equilibrium configurations for the nine DOPC and DOPC:DOPS systems investigated in this study, using area per lipid as an indicator of stability, occurs within about 50 ns (Figure 1A). Calcium−lipid binding patterns continue to evolve, however, until approximately 100 ns (Figure 1B). No further changes in these properties were observed after an additional 100 ns (200 ns total). Area per lipid and the corresponding bilayer thickness data for each system, time-averaged from 140 to 150 ns, are compiled in Table 2. Adding calcium ions to the solvent or PS to the bilayer causes a decrease in area per lipid and a corresponding increase in bilayer thickness, consistent with previous experimental observations[15] and simulations.[26]

(43) Humphrey, W.; Dalke, A.; Schulten, K. *J. Mol. Graphics* **1996**, *14*(1), 33–8.

Table 2. Variation in Bilayer Area Per Lipid and Thickness with Number of Calcium Ions and PS Molecules

	area per lipid (nm^2)			thickness, z_{P-P} (nm)		
PS	0 Ca	10 Ca	100 Ca	0 Ca	10 Ca	100 Ca
0	0.66	0.62	0.60	3.9	4.3	4.3
10	0.64	0.60	0.58	4.0	4.3	4.3
20	0.61	0.59	0.58	4.2	4.4	4.3

Mean values over the interval 140 to 150 ns of the simulations. Thickness is the distance along the bilayer normal between the planes defined by the phosphorus atoms in each leaflet of the bilayer. Standard deviations for the area per lipid values are <0.01.

Calcium Distribution in DOPC Bilayers. Calcium distribution profiles in pure DOPC bilayer systems containing 10 (Figure 2A) and 100 (Figure 2B) calcium ions show a single Ca^{2+} peak located between the headgroup phosphate and the backbone carbonyl peaks, consistent with neutron diffraction measurements.[20] In the 10-calcium system all of the calcium is found in this peak, but in the 100-calcium system a significant concentration of calcium in the bulk is observed, indicating that the calcium capacity for this 128-DOPC system saturates somewhere between 10 and 100 calcium ions.

Calcium Distribution in DOPC:DOPS Bilayers. Calcium distribution profiles in DOPC:DOPS (108:20) systems containing 10 (Figure 2C) and 100 (Figure 2D) calcium ions show a single Ca^{2+} peak in the pure DOPC leaflet of the bilayer (left side of diagrams in Figure 2), but the distribution is shifted to the DOPS carboxyl group in the mixed DOPC:DOPS leaflet (right side of Figure 2C and 2D). In the 10-calcium, mixed-lipid system, as with pure DOPC, all of the calcium is localized in the bilayer. In the 100-calcium system again there is a significant calcium concentration in the bulk, indicating that the calcium capacity for this mixed 128-lipid DOPC:DOPS bilayer, like that of the pure DOPC system, saturates between 10 and 100 calcium ions.

Calcium and Chloride Interfacial Distribution in DOPC and DOPC:DOPS. In the calcium-saturated DOPC and DOPC:DOPS systems, the calcium concentration reaches a maximum in the phosphate or carboxyl region of the bilayer interface, drops to a minimum at the solvent boundary, then rises again in the bulk medium (Figure 2B,D). This MD-simulated manifestation of the electric double layer[25,27,29] can be seen in more detail in Figure 3, which also elucidates the differences between the pure DOPC leaflet and the mixed DOPC:DOPS leaflet. At the DOPC-only interface (Figure 3A) the phosphate-localized calcium peak, the counteracting calcium and chloride profiles, and the exclusion of sodium from the headgroup region are straightforward. At the aqueous boundary of the mixed DOPC:DOPS leaflet on the other side of the bilayer (Figure 3B) the calcium and chloride peaks are distinct, but the calcium profile in the headgroup region traces a landscape complicated by the presence of the serine carboxyl groups, and the calcium is accompanied by a significantly greater amount of sodium than in the DOPC-only leaflet.

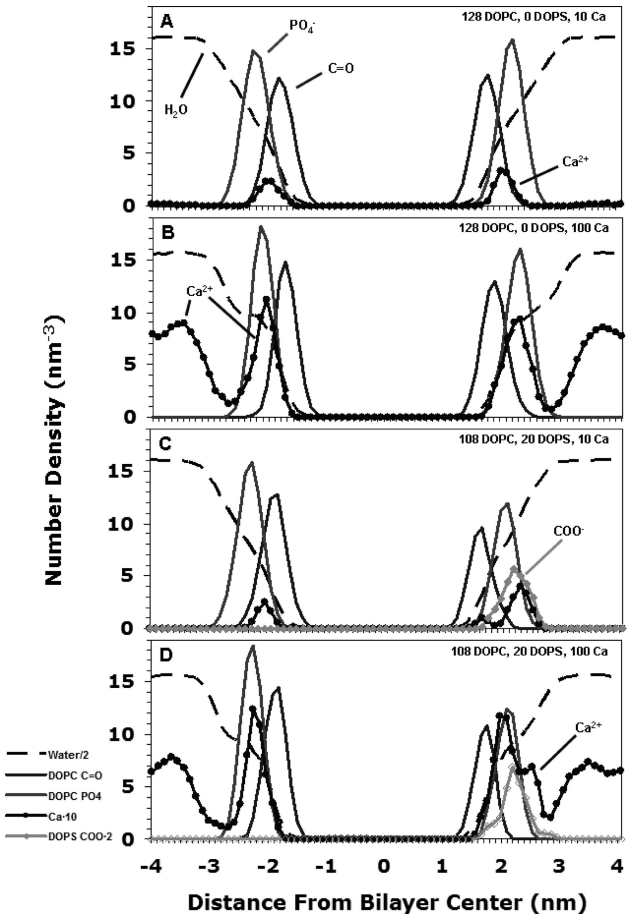

Figure 2. Number density (nm^{-3}) profiles for selected components of DOPC and DOPC:DOPS (108:20) bilayer systems containing 10 (A,C) and 100 (B,D) calcium ions and corresponding counter-ions (Table 1). For convenient scaling, calcium density is multiplied by 10, DOPS carboxyl density is multiplied by 2, and water density is divided by 2. The phosphate and carbonyl profiles are for the DOPC-associated residues. To simplify the diagram, the DOPS phosphates and carbonyls, which coincide almost exactly with their DOPC counterparts, are not shown. The plots are centered on the density minimum at the midpoint of the bilayer.

Calcium Density in DOPC and DOPC:DOPS Systems. To understand the calcium distribution in the DOPC:DOPS system in a more quantitative way, we consider next the concentration of calcium in the phosphate and carbonyl regions of the bilayer, defined in Table 3 and shown graphically in Figure 2. As shown in Table 3, the concentration of calcium in the phosphate and carbonyl regions of the DOPC-only leaflet (left side of Figure 2) is not significantly affected by the presence of PS in the opposite leaflet. In the DOPC:DOPS leaflet, however, increasing the fraction of PS increases the concentration of calcium in both the phosphate and carbonyl regions. (As shown in Figures 2 and 3, the PS carboxyl group lies almost entirely inside the phosphate distribution, so it is not tabulated separately here.)

Converting the atomic number densities in Table 3 to molar concentrations ($atom \cdot nm^{-3} \times 1.66 = mol \cdot L^{-1}$) permits comparison to physiological conditions and to previous analyses of calcium binding to phospholipid membranes. For the 10-calcium systems presented here, the concentration of calcium in the bulk solvent is essentially zero (Figure 2A, 2C), so we may consider the membrane calcium concentrations in these systems to lie near the lower limit of physiological calcium concentrations in the aqueous−membrane interface. Simplifying by taking values from the combined phosphate-carbonyl region in Table 3, we find interface calcium concentrations in the range 60−100 mM in the DOPC-only leaflet and 110−170 mM in the DOPC:DOPS leaflet. These values, and the distribution of calcium in the bilayer, are consistent with the model and measurements reported by

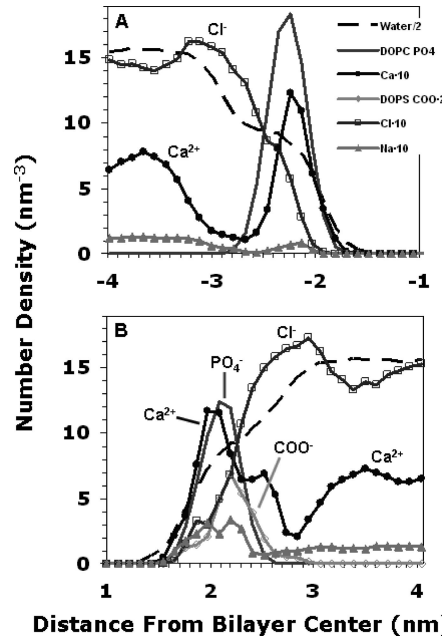

Figure 3. Number density (nm^{-3}) profiles for the interface regions of the DOPC-only (A) and DOPC:DOPS (B) leaflets of a DOPC:DOPS (128:20) asymmetric bilayer. The DOPC-only leaflet contains 64 DOPC. The DOPC:DOPS leaflet contains 44 DOPC and 20 DOPS. A and B are expanded views of the left side and right side, respectively, of Figure 2D. In addition to the scaling applied in Figure 2, the chloride and sodium densities are each multiplied by 10.

Table 3. Calcium Density in Phosphate and Carbonyl Regions of the Phospholipid Interface in the DOPC and DOPC:DOPS Leaflets[a]

	Ca^{2+} density (nm^{-3})			
	PO_4^{PC}		$PO_4^{PC:PS}$	
PS	10 Ca	100 Ca	10 Ca	100 Ca
0	0.07	0.41	0.08	0.36
10	0.08	0.37	0.08	0.44
20	0.05	0.42	0.13	0.56
	$C{=}O^{PC}$		$C{=}O^{PC:PS}$	
PS	10 Ca	100 Ca	10 Ca	100 Ca
0	0.07	0.34	0.08	0.32
10	0.08	0.32	0.08	0.35
20	0.04	0.36	0.09	0.43
	$PO_4{+}C{=}O^{PC}$		$PO_4{+}C{=}O^{PC:PS}$	
PS	10 Ca	100 Ca	10 Ca	100 Ca
0	0.05	0.31	0.06	0.28
10	0.06	0.29	0.06	0.34
20	0.04	0.32	0.10	0.46

[a] Densities are the time-averaged values (140−150 ns) of the number of calcium ions in the rectangular volumes defined by the maximum and minimum position along the bilayer normal of any of the oxygen atoms connected to phosphorus (PO_4 region) and any of the carbonyl oxygens (C=O region) − the boundaries on either side of the peaks in Figure 2. Phosphate and carbonyl regions overlap, and the PC phosphate, PS phosphate, and PS carboxyl regions are essentially coincident (see Figure 2). PO_4 and C=O with superscripts PC and PC:PS refer to the phosphate and carbonyl regions in the PC-only leaflet (Figure 2, left side) and the mixed PC:PS leaflet (Figure 2, right side), respectively. $PO_4{+}C{=}O$ is the combined phosphate and carbonyl region in each case, defined by the extreme positions of phosphate and carbonyl oxygens.

Table 4. Water Density in Phosphate, Carbonyl, and Choline Regions of the Phospholipid Interface[a]

	H_2O density (nm^{-3})					
	PO_4^{PC}			$PO_4^{PC:PS}$		
PS	0 Ca	10 Ca	100 Ca	0 Ca	10 Ca	100 Ca
0	17.1	14.3	15.0	16.1	14.0	15.3
10	16.3	16.2	14.5	15.2	15.3	14.9
20	15.1	15.5	14.9	15.7	16.3	14.7
	$C{=}O^{PC}$			$C{=}O^{PC:PS}$		
PS	0 Ca	10 Ca	100 Ca	0 Ca	10 Ca	100 Ca
0	9.4	7.4	9.0	9.2	8.2	8.9
10	9.4	9.1	8.8	8.1	7.9	8.7
20	8.3	9.4	8.8	8.1	8.1	8.1
	$PO_4{+}C{=}O^{PC}$			$PO_4{+}C{=}O^{PC:PS}$		
PS	0 Ca	10 Ca	100 Ca	0 Ca	10 Ca	100 Ca
0	14.0	11.3	11.5	13.0	11.1	12.1
10	13.2	13.0	11.3	12.1	12.1	11.4
20	12.2	12.4	11.2	12.4	12.5	12.0
	$choline^{PC}$			$choline^{PC:PS}$		
PS	0 Ca	10 Ca	100 Ca	0 Ca	10 Ca	100 Ca
0	18.3	17.0	17.5	17.6	16.8	17.6
10	17.8	16.9	17.0	19.5	18.0	17.7
20	18.5	18.0	17.5	16.6	19.2	18.6

[a] Densities and regions are defined as in Table 3, for water molecules rather than for calcium ions. Because the range of motion of the choline atoms is essentially coincident with the range covered by all of the head group atoms back to the glycerol backbone, the density of water in the choline region and the density of water for the complete head group region differ by less than 10%.

Seelig[17]—for $[Ca^{2+}]_{bulk} = 1$ mM, $[Ca^{2+}]_{bound}$ (confined within a stratum of 1 nm thickness) = 167 mM and with the simulation results reported by Pedersen et al. for charged phospholipid bilayers.[9]

Experimental studies suggest a surface calcium ion concentration that is 3 to 30 times higher than the bulk concentration,[17,32] and that this high surface concentration, not preferential binding to PS, accounts for greater binding of Ca to PC:PS relative to pure PC. The small size of our systems, in which a single calcium ion in the bulk solvent region corresponds to a concentration of about 20 mM, does not permit detection of this surface charge layer. The 100-calcium systems are clearly well beyond membrane binding site saturation and physiological conditions. The bulk calcium concentration in these systems is about 1.25 M, and the concentration in the phosphate-carbonyl region, again from Table 3, ranges from 470 mM to 760 mM.

To confirm that the number of solvent molecules is not a limiting factor, we ran additional simulations under identical conditions but with approximately 120 H_2O per lipid instead of 33−35 H_2O per lipid. The density profiles and binding patterns were essentially unchanged, and, even with this increased amount of water, none of the calcium ions left the interface to become part of the bulk solvent region.

Water Density in DOPC and DOPC:DOPS Systems. Experimental studies indicate that calcium binding to phospholipid bilayers is endothermic and entropy-driven, and that the entropy increase results at least in part from the displacement of interfacial water by calcium.[18,32] In Table 4 we see this effect most clearly by comparing the water densities in the DOPC-only systems with 0 and 10 calcium ions. In the 100-calcium systems, the interfacial water concentration is higher because the additional calcium in the membrane brings with it additional waters of hydration. The effects of calcium and of the PS:PC ratio on water density distributions in the mixed bilayer DOPC:DOPS systems are more complex because of the interactions of packing configurations and electrostatics, and simulations at intermediate calcium levels and PS:PC fractions will be required for the development of a more systematic analysis. Specifically, although our simulations provide a first-order picture of the partitioning of calcium in these mixed bilayers, the time course of calcium coordination indicates that even at 200 ns the systems are not yet fully stable in terms of the calcium distribution (and thus the water distribution) among the various binding sites. Conclusions about the extent of calcium-driven dehydration of the bilayer and the distribution of water in the membrane at equilibrium will require simulations that go beyond 200 ns.

Bound, Interface, and Bulk Calcium. In addition to the spatial distributions for calcium described above, we also analyzed the proximity of calcium to phospholipid binding sites (the electronegative phosphatidyl and carbonyl oxygen atoms). We find that, for the 10-calcium systems, almost all of the calcium ions are bound to a lipid (located within 0.3 nm of a phosphatidyl or carbonyl oxygen), as previously reported for PC bilayers,[26] and that PS in the bilayer increases the fraction of lipid-bound calcium (see Supporting Information Table 1). The attractive effect of PS is clearly evident in the saturated, 100-calcium systems as well. These calcium-saturated bilayers also contain more calcium ions in the interfacial region that are not bound to lipid, and which are therefore more fully hydrated, consistent with the higher interfacial water densities in 100-calcium systems noted above.

A detailed breakdown of the distribution of bound calcium in DOPC and DOPC:DOPS bilayers is presented in Table 5. Not only does the PS carboxyl bind a significant percentage of the total bound calcium, in agreement with previous simulations of anionic phospholipid bilayers,[9] it also dominates the DOPS intramolecular calcium binding space. In the 10-calcium, 20-PS system, the PS carboxyls account for half of the total calcium binding sites, and no calciums are found in binding proximity to the PS phosphate or PS carbonyl sites. Low levels of PS phosphate and PS carbonyl binding are observed in the 100-calcium system. The distribution of phosphate and carbonyl binding in the DOPC-only system (0 PS) is consistent with infrared spectroscopic evidence for PC vesicles at high calcium/lipid molar ratios.[18]

Calorimetry data for DOPC:DOPS vesicles with PS/PC = 0.11 suggests that calcium, at calcium/lipid molar ratios less than 0.1, binds preferentially to PS, then, at higher calcium concentrations, to PC.[32] Since our 10-calcium, 20-PS DOPC:DOPS systems have PS/(PC+PS) = 0.16 (but with an asymmetric distribution between the two leaflets of the bilayer) and a calcium/lipid molar ratio of about 0.08, the calorimetric evidence would lead us to expect that we are in the range where both PS and PC binding is occurring, and that is what we see (Tables 3 and 5).

Graphical representations of the radial distribution functions for calcium and the phospholipid binding sites (carbonyl, phosphatidyl, and carboxyl oxygens) in pure DOPC (Figure 4A) and mixed DOPC:DOPS bilayers (Figure 4B) confirm the specificity of the binding relationships presented in tabular form above. Note in particular the very strong coordination with the PS carboxyl relative to PC carbonyl and phosphatidyl oxygens and the absence of coordination with other PS oxygens (Figure 4B). When the number of calcium ions is increased from 10 (Figure 4) to 100 (not shown), PS carbonyl and phosphate coordination peaks appear, but at lower magnitudes than the

Table 5. Equilibrium Calcium Binding in DOPC and DOPC:DOPS Systems[a]

	phosphate-, carbonyl-, and carboxyl-bound Ca^{2+} (<0.3 nm), 140−150 ns											
	PC phosphate		PC carbonyl		PS phosphate		PS carbonyl		PS carboxyl		total Ca^{2+} pairs	
PS	10 Ca	100 Ca	10 Ca	100 Ca	10 Ca	100 Ca	10 Ca	100 Ca	10 Ca	100 Ca	10 Ca	100 Ca
0	12.8	96.0	11.9	46.7							24.7	142.7
20	10.9	65.2	8.2	46.7	0.0	6.9	0.0	5.2	18.4	34.5	37.5	158.5

[a] A bound calcium-lipid pair is recorded for each occurrence of a calcium ion located within 0.3 nm of a lipid binding site (phosphatidyl, carbonyl, or carboxyl oxygen). One calcium ion may be bound to multiple lipid binding sites and may thus be associated with multiple bound pairs. Data are mean values of the number of bound pairs for each group averaged over the interval 140 to 150 ns.

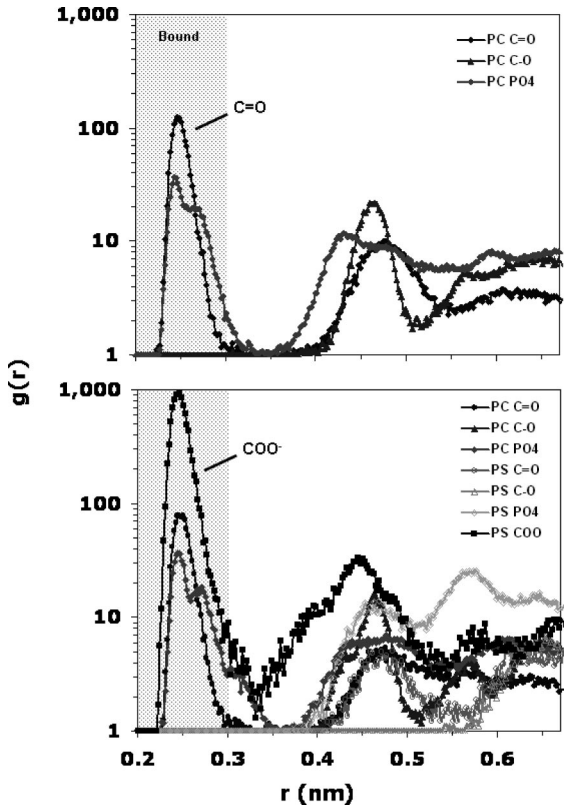

Figure 4. Radial distribution functions from equilibrated pure DOPC and mixed DOPC:DOPS (108:20) systems with 10 Ca^{2+}, time-averaged from 140 to 150 ns, for calcium and phospholipid binding sites (C═O: glycerol backbone carbonyl oxygens; C−O: backbone ether oxygens; PO4: oxygens bonded to phosphorus; COO: serine carboxyl oxygens). $g(r)$ values are plotted on a log scale to facilitate visualization of the secondary associations at radial separations greater than 0.3 nm. Bound calcium regions (≤0.3 nm) are shaded.

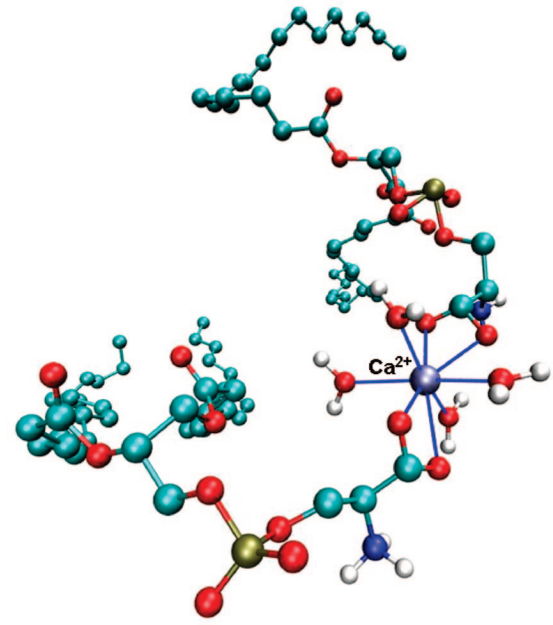

Figure 5. Calcium−DOPS−water complex from an equilibrated DOPC:DOPS (108:20) system. Calcium binds to DOPS and water with a stoichiometric ratio of 1:2:4. Blue lines connect calcium and atoms within 0.3 nm (oxygens from water and the DOPS carboxyl groups). Violet: Ca; red: O; white: H; teal: C; blue: N; gold: P.

corresponding PC carbonyl and phosphate peaks, consistent with the data in Table 5.

Calcium−PS Complex. Experimental evidence for a calcium/PS stoichiometric ratio of 1:2[12,13,15] is supported by structures such as the representative snapshot of a $Ca(PS)_2(H_2O)_4$ complex shown in Figure 5. In this ion−molecular assembly we see the replacement of solvating water in the lipid headgroup by calcium, and the concomitant partial dehydration of the calcium water shell (calcium coordinates 8−9 water molecules[44,45]), which follow from the enthalpic and entropic considerations mentioned above in the discussion of water density. A movie showing the formation of calcium-carboxyl oxygen complexes like the one in Figure 5 is provided as Supporting Information. Calcium-carboxyl oxygen coordination numbers (Supporting Information Table 2) show the prevalence of 3- and 4-oxygen structures ($Ca(PS)_2$) in the 10-calcium systems. With 100 calcium ions, the binding affinity between the multiplicity of calcium ions and the limited number of serine carboxyl oxygens dominates over the tendency to form the coordinated dimer. Although no calcium-coordinated complexes involving both carboxyl oxygens and phosphatidyl oxygens (from PC or PS) were observed during the 140−150 ns sampling period, and there were no instances of calcium coordinating phosphatidyl oxygens from two phospholipids, PC oxygens form a variety of associations with calcium; for example, complexes with three carbonyl oxygens (from three different DOPC molecules), with two carbonyl oxygens and a phosphatidyl oxygen (again from three different DOPC molecules), and with carboxyl (DOPS) and carbonyl (DOPC) oxygens detected (not shown). The lifetime of these complexes and their effect on the diffusion of calcium and phospholipids in the membrane will be addressed in future work.

Calcium and Sodium in the Bilayer Interface. The sodium ions included as counterions for the PS carboxyl groups contribute, along with calcium ions and the electronegative lipid binding sites, to the electrostatics and energetics of the bilayer. Although the interactions of these components with sodium ions are complex, some general patterns can be discerned from shifts in mean sodium concentration (Supporting Information Table 3) and distribution peaks (Figure 6) in the membrane interface. As

(44) Palinkas, G.; Heinzinger, K. *Chem. Phys. Lett.* **1986**, *126*(3−4), 251–254.
(45) Megyes, T.; Bako, I.; Balint, S.; Grosz, T.; Radnai, T. *J. Mol. Liq.* **2006**, *129*(1−2), 63–74.

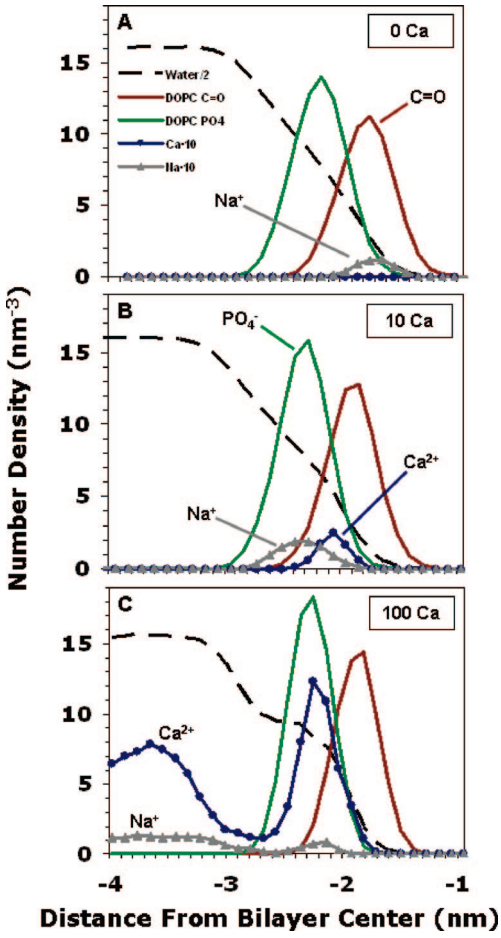

Figure 6. Number density (nm^{-3}) profiles, including sodium, for the DOPC-only leaflet of a DOPC:DOPS (128:20) asymmetric bilayer, with some components not shown for clarity. B and C are expanded views of the left sides of Figure 2C,D, respectively. As in Figure 3, calcium and sodium densities are each multiplied by 10, and water density is divided by 2.

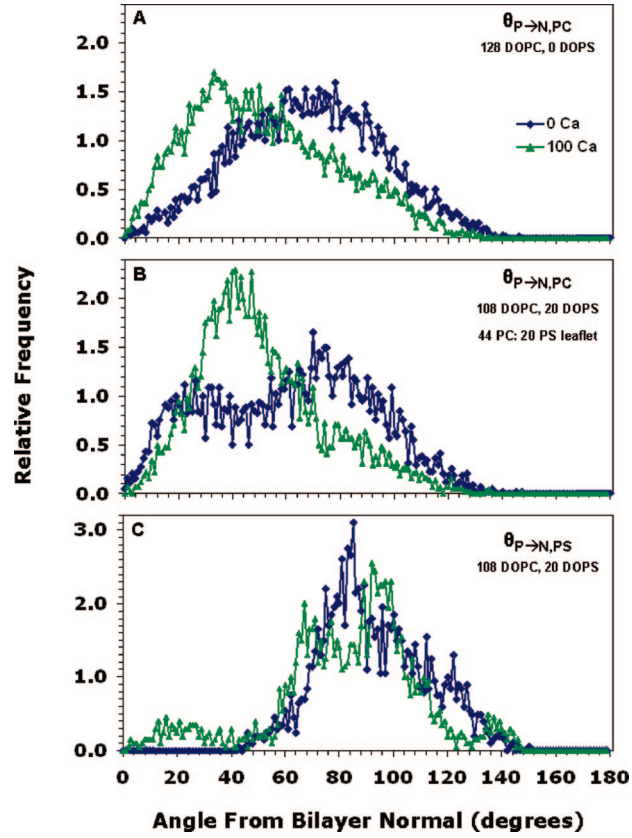

Figure 7. Calcium-induced changes in PC and PS headgroup orientation in DOPC and DOPC:DOPS bilayers. Distribution of headgroup P→N dipole angles relative to the bilayer normal based on atomic coordinates from (A) 128 DOPC molecules in a pure DOPC bilayer, (B) 44 DOPC molecules in the DOPC-only leaflet of a DOPC:DOPS (128:20) bilayer, (C) 20 DOPS molecules in the mixed DOPC:DOPS leaflet of a DOPC:DOPS (108:20) bilayer. Each panel shows distributions from simulations containing zero (diamond symbol) and 100 (triangle symbol) calcium ions. Data was sampled every 100 ps between 140 and 150 ns.

shown in Figure 6A, and consistent with earlier studies,[25,46,47] sodium penetrates to the carbonyl level of a DOPC-only leaflet of a DOPC:DOPS (108:20) bilayer. In the 10-calcium system, the presence of calcium ions in the phosphate region is associated with an outward shift in the peak of the sodium ion distribution, away from the carbonyl region (Figure 6B), while at the same time facilitating an increase in the number of sodium ions in the interface. In the 100-calcium system this increased sodium is expelled into the bulk solvent (Figure 6C), consistent with experimental observations[15] and simulations of other phospholipid systems.[9]

On the DOPC:DOPS side of the bilayer, sodium is found in the phosphate region, chaperoned by the carboxyl groups in the DOPC:DOPS (108:20) system, even with 100 calcium (Figure 3B). With only 10 PS in the leaflet instead of 20; however, sodium is excluded from the interface of a 100-calcium system (not shown), just as it is from the DOPC-only leaflet (Figure 6C).

The effects of the gratuitous presence of sodium ions on both sides of the bilayer, a consequence of the periodic boundary conditions applied to these systems, may be questioned, since these ions are added to the system as counter-ions to the ionized PS residues, which are confined to one leaflet of the bilayer. This is a limitation imposed by system size and computational resources. It could be addressed by a double-bilayer system, in which the sodium counter-ions for DOPS would be confined to the inner compartment, but this would also require assumptions (or knowledge not yet obtained) regarding the equilibrium calcium ion concentration on the two sides of the bilayer and systems large enough to accommodate the appropriate numbers of ions in each compartment at physiological concentrations.

Calcium and PC and PS Headgroup Dipole Angle. The effects of monovalent and divalent ion binding on the phospholipid headgroup dipole angle have been studied experimentally[22] and more recently with the tools of MD.[26,29,31] Here we examine calcium-induced changes in the PC and PS headgroup dipole angle distribution in DOPC and mixed DOPC:DOPS bilayers.

In the pure DOPC system, the broad PC P→ N dipole angle distribution peaks at approximately 78 degrees from the bilayer normal (the choline nitrogen is on the average lifted about 12° out of the plane of the bilayer in the direction of the bulk solvent (Figure 7A). In the same system after equilibration with 100 calcium ions, the headgroup dipole angle peak shifts to about 43° (Figure 7A), a very large change. In a 10-calcium system (not shown), we observe an intermediate value, about 64°, for the peak of the dipole angle distribution.

In the PC:PS leaflet of a DOPC:DOPS (108:20) system, the PC dipole angle distribution is bimodal, with a larger peak at about 76° and a smaller peak at about 25° (Figure 7B). This "splitting" of the PC headgroup dipole angle arises from interactions with neighboring PS head groups. The PC dipole

(46) Gurtovenko, A. A. *J. Chem. Phys.* **2005**, *122*(24), 244902.
(47) Lee, S. J.; Song, Y.; Baker, N. A. *Biophys. J.* **2008**, *94*(9), 3565–76.

angle distribution in the PC-only leaflet of the mixed, asymmetric DOPC:DOPS (108:20) bilayer is essentially identical to the distribution in the pure DOPC system. In the presence of 100 calcium ions, a single PC dipole angle peak is observed at about 44° (Figure 7B). As might be expected, we observe intermediate values for the PC dipole angle distribution in a 10-calcium DOPC:DOPS (108:20) system, with peaks at 72° and 44° (not shown).

For comparison we looked also at the effect of calcium on the P→N vector component of the headgroup dipole angle for PS in the DOPC:DOPS (108:20) system. We refer to this as the PS headgroup dipole angle, although we are ignoring the contribution of the negatively charged carboxyl group. A dominant peak in the distribution is observed at about 85° in the absence of calcium (Figure 7C). Interestingly, in a 100-calcium system, the PS headgroup dipole angle distribution becomes bimodal, with peaks at about 97° and about 70° (Figure 7C), suggesting, along with the results for the PC dipole angle, complex and subtle adjustments in conformation and aggregation among the phospholipids in a mixed zwitterionic/anionic bilayer in response to local changes in monovalent and divalent cation concentrations. Again, the 10-calcium system dipole angle distribution is intermediate, with a single peak shifted to about 93°, and no obvious second peak (not shown). It should be emphasized that these are not static alignments. The orientation of any given individual headgroup dipole in these thermally agitated bilayer systems, all above the phospholipid melting temperatures, ranges over tens of degrees within tens of picoseconds.

4. Conclusions

MD simulations of mixed, zwitterionic-anionic, asymmetrically arranged DOPC:DOPS bilayers with monovalent and divalent cations are consistent with experimental observations and with previously reported results for simulations of simpler phospholipid systems. In addition to confirming for the DOPC:DOPS system the area-decreasing, thickness-increasing, interface-dehydrating effects of calcium ions, the greater affinity of phospholipid binding sites for calcium relative to sodium, the greater affinity of calcium for PS carboxyl sites relative to phosphate and carbonyl sites, and the calcium-induced rotation of the PC headgroup dipole toward the solvent, we have also identified some new features of these model systems.

Area per lipid, often used as an indicator of attainment of a thermal and electrostatic equilibrium in simulations of lipid bilayer systems, is misleading in the case of DOPC:DOPS with calcium, for which the area per lipid stabilizes after about 50 ns, but the establishment of a stable number of coordinated calcium−lipid pairs, and the associated ion−lipid structural rearrangements, takes at least 100 ns.

For a 128-lipid DOPC:DOPS system, saturation of the calcium capacity of the bilayer occurs between 10 and 100 calcium ions.

The PC headgroup dipole angle distribution in PC:PS bilayers is bimodal, an effect of the interaction between the anionic PS and the zwitterionic PC, and this distribution can be further modulated by varying the number of calcium ions in the system. Atomically local binding profiles for anionic versus zwitterionic phospholipids and their combinations, with monovalent and divalent counter-ions, may have significant consequences for membrane lipid and protein aggregations.

The ion models from the GroMACS ffgmx topology database used here have limitations arising from their nonpolarizability,[47] which we accept because of computational resource limits. In particular, their performance in aqueous and nonaqueous systems may differ markedly; adjusting the force field parameters for one environment can cause unsatisfactory behavior in another.[48] Because calcium in the interface region remains at least partially hydrated (with some water oxygens replaced by carboxyl, carbonyl, and phosphatidyl oxygens), and because the coordination number and geometry of this lipid-bound calcium is similar to that of fully hydrated calcium,[44] we think it is reasonable to expect that the calcium model does not introduce unacceptable inaccuracies in these phospholipid bilayer systems. This expectation is supported by the correspondence of our results with experimental studies.

From another perspective, this work underlines the necessity for improvement of the accuracy of the atomic-level interactions. Continuing and extending the development of molecular models and mechanisms for membrane fusion, budding, invagination, ruffling, pseudopod extension, and other remodeling processes, and for electroporation and electric field-driven and mechanical restructuring of the membrane, will require taking into account, as we have done here, the effects of monovalent and divalent cations, calcium in particular, but not only calcium, in heterogeneous asymmetric bilayers. But beyond this, to begin to answer questions that approach the level of cell physiology, functionally if not dimensionally, a simulation of ions at the phospholipid interface must properly represent not only systems at equilibrium but also those with large spatial (nanometer scale) and temporal (nanosecond scale) ion concentration gradients, such as those encountered, for example, when plasma membrane ion channels are activated or when the contents of intracellular calcium compartments are released. Continuum properties such as diffusion coefficients, binding constants, and stoichiometries, which guide us at larger scales, are less relevant in this dynamic regime than the precision in local electrostatics and van der Waals forces and in bond angles and dimensions, which ensures that molecular velocities and residence times reflect and respect the complexities of hydration, hydrogen bonding, and hydrophobic interactions in the stereospecifically complex, low-density (water), highly nonuniform electrical permittivity environment of the membrane interface.

Acknowledgment. We thank Rainer Böckmann and Peter Tieleman for stimulating discussions. Computing resources were provided by the USC Center for High Performance Computing and Communications. This work was made possible in part by support from the Air Force Office of Scientific Research. P.T.V. and M.J.Z. are supported by MOSIS, Information Sciences Institute, Viterbi School of Engineering, University of Southern California.

Supporting Information Available: Additional tables and a video showing the formation of calcium−phospholipid complexes in a phospholipid bilayer. This material is available free of charge via the Internet at http://pubs.acs.org.

LA8025057

(48) Warshel, A.; Kato, M.; Pisliakov, A. V. *J. Chem. Theory Comput.* **2007**, *3*(6), 2034–2045.